

Carbonization of polyacrylonitrile-based fibers under defined tensile load: influence on shrinkage behavior, microstructure, and mechanical properties

Patrick Gutmann, Judith Moosburger-Will, Samet Kurt, Yinqiao Xu, Siegfried R. Horn

Angaben zur Veröffentlichung / Publication details:

Gutmann, Patrick, Judith Moosburger-Will, Samet Kurt, Yinqiao Xu, and Siegfried R. Horn. 2019. "Carbonization of polyacrylonitrile-based fibers under defined tensile load: influence on shrinkage behavior, microstructure, and mechanical properties." *Polymer Degradation and Stability* 163: 174-84.
<https://doi.org/10.1016/j.polymdegradstab.2019.03.007>.

Carbonization of polyacrylonitrile-based fibers under defined tensile load: influence on shrinkage behavior, microstructure, and mechanical properties

Patrick Gutmann^{a,*}, Judith Moosburger-Will^b, Samet Kurt^a, Yinqiao Xu^a, Siegfried Horn^{a,b}

^a Experimental Physics II, Institute of Physics, University of Augsburg, 86135 Augsburg, Germany

^b Institute of Materials Resource Management, University of Augsburg, 86135 Augsburg, Germany

* *corresponding author*, patrick.gutmann@physik.uni-augsburg.de

Abstract

The influence of temperature and tensile mechanical load during carbonization of stabilized polyacrylonitrile fibers on the shrinkage behavior, the crystalline parameters and the mechanical properties of the resulting fibers is investigated. To this end, a newly developed experimental setup enables a defined heat treatment of fiber bundles up to a temperature of 1200°C under control of tensile load. The attachment devices for the fiber bundles are located in the hot zone of the furnace. Additionally, carbonization treatments up to 1600°C without application of load are performed.

Three characteristic temperature regions of the carbonization process are identified.

Between 250°C and 450°C the still ductile fibers contain rests of the polyacrylonitrile phase experiencing stabilization reactions. Stacked, heterocyclic planar structures grow due to molecular crosslinking. Between 450°C and 1000°C graphite-like turbostratic carbon is formed. Crystallites grow laterally, crystallinity increases, and the material becomes brittle. Above 1000°C a pronounced increase in stacking height, lateral crystallite size and crystallinity occurs, while the interlayer distance decreases. Mechanical properties reach the values typical for commercial carbon fibers. Application of a tensile stress during carbonization influences fiber dimensions at temperatures between 250°C and 450°C, where the material shows ductile behavior. Shrinkage in fiber direction is hindered and radial shrinkage is favored. At temperatures above 1000°C, crystalline parameters and mechanical properties of the resulting carbon fibers depend on the applied tensile stress. Carbonization without tensile stress results in significantly lower mechanical properties. The impact of heat treatment temperature and applied stress on carbon fiber properties demonstrate the possibility of a defined tailoring of fiber characteristics.

Keywords:

Carbon Fiber, Carbonization, Thermomechanical Analysis, Elongation Behavior, Mechanical Testing, Heat Treatment, Structural Analysis, Polyacrylonitrile

1. Introduction

As carbon fiber reinforced materials play an increasingly important role in the field of lightweight construction and high-performance materials, throughout the last 50 years great efforts have been undertaken to investigate their production, properties, and fields of application [1–7]. During the industrial manufacturing process of carbon fibers, a tow of endless fiber filaments is led through various sections of heat treatment. First the precursor polyacrylonitrile (PAN) fibers are stabilized

under oxidative atmosphere at temperatures between 200°C and 300°C to generate a structure suitable for high temperature treatment [8–11]. In a next step these stabilized fibers are carbonized at temperatures up to 1600°C under inert (nitrogen) atmosphere. A material containing typically more than 98wt% carbon is produced. The crystalline parts of this semi-crystalline material show a turbostratic graphitic microstructure, in which graphite-like layers are stacked with random orientation relative to each other [12]. During the carbonization process heteroatoms like nitrogen, oxygen, and hydrogen are eliminated from the structure, which results in the emission of volatile products like HCN, NH₃, CO₂, CO, H₂, N₂, H₂O, hydrocarbons, and nitriles [13, 14]. An optional subsequent graphitization step at temperatures up to 3000°C, usually under noble gas atmosphere, results in a fiber that contains about 99wt% carbon [10, 15, 16].

In the initial stages of carbonization (300°C < T < 600°C) intermolecular dehydrogenation and deoxygenation is assumed to take place [13, 16, 17]. In this process heterocyclic ladder-like polymer molecules, which are considered to be formed during stabilization [13, 18–20], perform crosslinking and establish larger planar heterocyclic structures. At temperatures above 600°C denitrogenation occurs. This is indicated by strong emission of N₂, which becomes maximal around 900°C and signals condensation reactions of existing structures, leading to the lateral growth of graphite-like ring systems [13, 14, 17, 21, 22]. An increase of stacking height of such graphite-like crystallites is observed at temperatures up to 2200°C [23].

The described chemical and structural modifications involve a severe mass-loss, especially in the temperature range between 300 and 500°C [16, 24], as well as an axial and radial shrinkage of the fibers [16, 25, 26]. Shrinkage is reported to be affected by mechanical tensile load on the fibers, specifically at temperatures below 500°C [16]. It is also reported that the application of mechanical tensile load during carbonization can improve the mechanical properties of the fibers [27, 28].

Thus, the effect of tensile load during carbonization on fiber properties is of high interest and has already been the topic of several publications. While some publications refer to the continuous fiber production process close to industrial manufacturing [29–31], others use a batch process [32–37]. Here the free choice of temperature, atmosphere, and stress program, which allows for the measurement of the temperature-dependent evolution of material parameters, outweighs the fact that this process is further away from the industrial process. Depending on the parameters addressed, those batch processes are using conventional furnaces [32, 34] or alternative concepts like infrared radiation to heat the fiber bundles [37].

To accurately measure the induced length change of the fibers during carbonization, a homogenous heat profile over the clamped fiber length must be guaranteed. Since the fibers are nonconducting in the beginning of the carbonization process, direct heating by an electric current is not possible [35, 36]. Therefore, the fiber bundle must be clamped within the hot section of a furnace. To submit fibers to thermal treatment under mechanical load, Ref. [25] modified a TMA (Thermomechanical Analysis) to clamp approximately 3000 fibers of approximately 20mm length using a screwed fastening. To investigate the carbonization process under constant load, Refs. [29, 32, 38] realized a setup with loading by different weights.

This publication presents to our knowledge for the first time an experimental setup to precisely measure the length change of a 6k fiber tow during the carbonization process under variable load [39]. The setup combines a newly developed method for fiber-clamping within the homogeneous hot section of the furnace and the use of a mechanical testing machine to measure the length change of

the fiber bundle at a precisely defined tensile load. The carbonization can be performed under well controlled atmospheres.

The publication describes the carbonization treatment of PAN-based stabilized fibers under different mechanical tensile loads for temperatures up to 1600°C. The temperature and tension dependent shrinkage of the fibers is correlated to changes of diameter, crystalline parameters and mechanical properties of the fibers.

2. Experimental

2.1. Carbonization Setup

In Figure 1 the developed experimental setup is shown schematically (left) and as a photograph (right). The components are labelled by the numbers (1) to (12). The setup is composed of three main systems, namely the tensile system, the vacuum system, and the heating system.

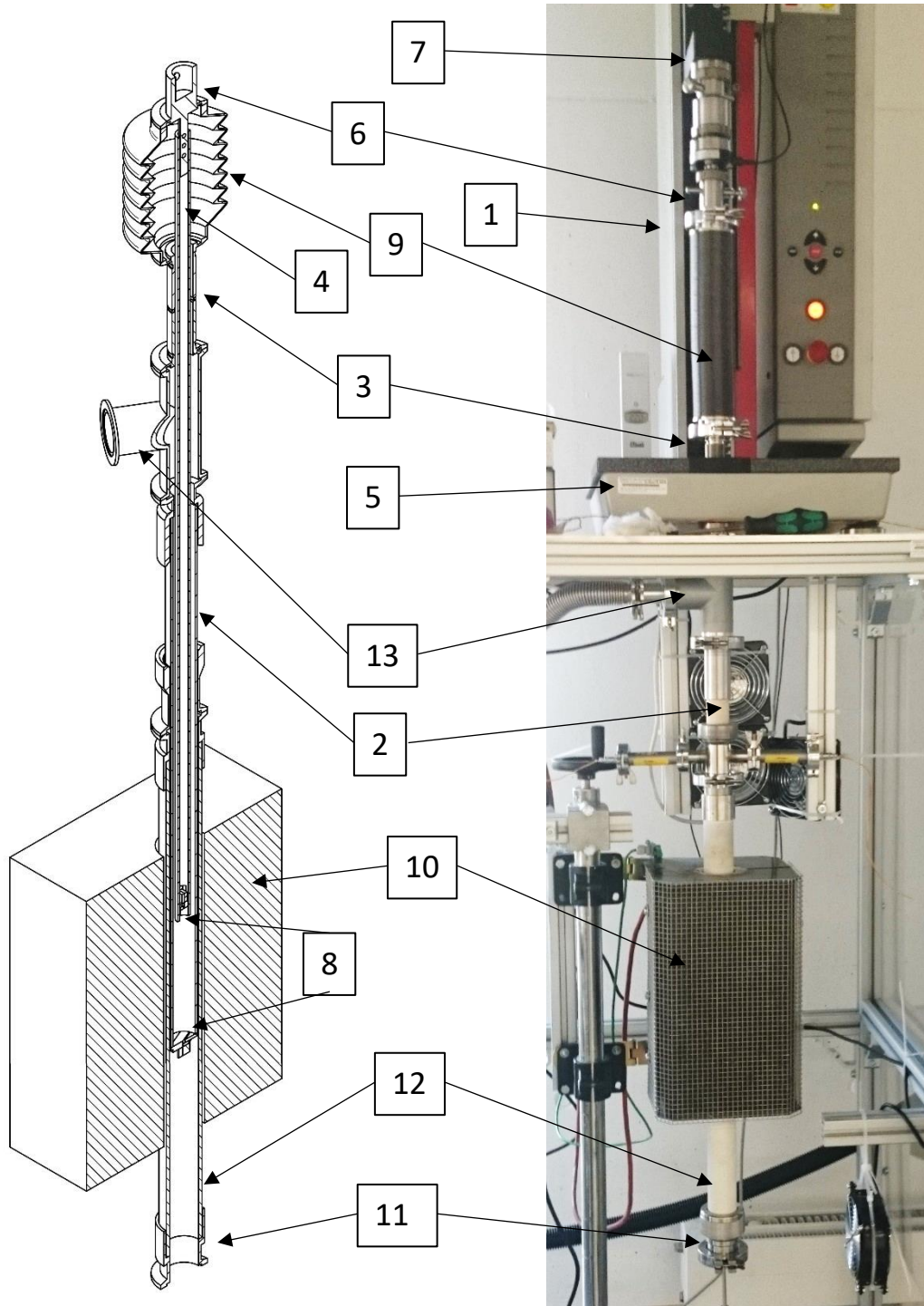


Figure 1: Schematic of the setup for high temperature treatment of fiber bundles (left) and photograph of the setup ready-to-use (right). The different components of the setup are labelled by the numbers (1) to (12).

For the **tensile system**, a tensile testing machine ZwickiLine Z0.5 (1) using a 500N load cell of the type X-force P is connected to a system of two concentrically assembled ceramic tubes. The outer tube (2) is fixed at its upper end to a T-branch (13) and a flange (3) immovably screwed from below into the base-plate (5) of the tensile testing machine. The inner tube (4) is lead through the base-plate from above and connected by an adapter (6) at its upper end to the force cell which is fixed to the traverse of the testing machine (7). The inner tube can, therefore, be moved by the testing machine. The fiber sample is fixed between the lower ends of these two tubes (8) so that the force generated by the tensile testing machine is transferred to the sample. The aim is to completely attach the fiber bundle within the hot section of the oven so that transition zones of the tested fibers, i.e. zones with varying material properties due to varying heat treatment, are avoided. Figure 2 (a) – (e) shows a newly developed system for fixing the fibers to the ends of the tubes, which is resistant to the carbonization temperatures.

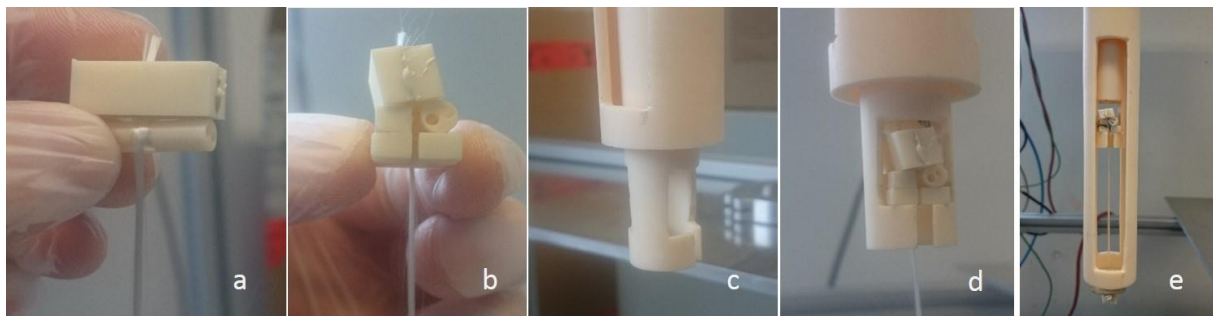


Figure 2: Mounting system for connecting the fiber bundle with the tensile system.

The fiber bundle is fixed by ceramic glue between two ceramic plates. Possible slippage of the inner fibers of the bundle, which are not in direct contact with the glue, is impeded by an additional winding of the fiber bundle around a small ceramic rod (a). This way the friction between the outer and the inner fibers prevents any kind of slippage. The same fixation is used at both ends of the fiber bundle. The two ends of the bundle must be wrapped around the respective rod in opposite directions. In this way all fibers of the fiber bundle are parallel to each other. The two systems consisting of ceramic plates and ceramic rods are located on ceramic mounting devices (b). Such a mounting device consists of two parts: a plate with a notch guiding the bundle and a spacer slightly higher than the ceramic rod to protect the wound fibers. The mounting device at the one end of the bundle is then placed into a cavity at the lower end of the inner tube (c, d). The mounting device at the other end of the fiber bundle is contacted to the lower rim of the outer tube (e) (c.f. (8) in Figure 1). Consequently, the fibers can be stressed by opposite movement of the inner tube relative to the outer tube. Fiber bundles up to the length of the homogenous zone of the furnace, which is about 150mm, can be treated in this setup.

The **vacuum system** enables treatment of PAN-based fibers in an inert atmosphere. A vacuum tight space is achieved by a.) placing a bellows (9) in Figure 1) between the base plate and the force cell at the traverse of the tensile testing machine, so that the part of the experimental setup above the base plate is closed and b.) mounting a further protective ceramic tube (12) around the outer tube with a specially designed flare type fitting at the lower end of the tube system. The flange of this fitting (11) connects to a gas handling system equipped with one or several mass flow controllers, that enable precise mixtures of pure gases at a defined flow rate. The measurements presented used 250sccm of pure nitrogen. A gas outlet consists of a capillary to avoid back-diffusion and is installed at the branch connection (13). The system is evacuated by a vacuum pump.

The **heating system** allows for defined temperature control at the position of the clamped fiber sample. Any type of tube furnace ((10) in Figure 1) can be mounted around the ceramic tubes and can be positioned in a way that the spatial temperature distribution in the region of the specimen is homogenous. Currently a conventional tube furnace, i.e. the model LOBA 1200-45-300-1 from HTM Reetz GmbH, is employed. It is equipped with a FeCrAl resistance wire that allows for a maximal temperature of around 1200°C and heating rates of maximal 20K/min.

Finally, the following sensors are installed. The pressure inside the system is measured by a vacuum gauge near the T-branch connection, as due to the bellow it has an impact on the tensile force on the fiber specimen and therefore must be kept constant. At both ends of the clamped fiber bundle and in its middle region thermoelectric sensors (Type K connected to a Meilhaus RedLab multichannel temperature analyzer) are installed to control and monitor the axial homogeneity of the temperature distribution and to measure the exact temperature right at the specimen position. There might be an offset between the temperature measured by the oven's temperature sensor and the temperature measured at the sample position due to thermal inertia.

Length and force measurement were calibrated in the following way.

As the tensile system is subject to thermal expansion, the thermally induced displacements of the mounting devices were measured for several traverse positions and for suitable heating cycles. In the parameter range used for our experiments (for a typical sample length of 100mm) the maximal thermally induced change of the mounting device positions is 0.2%. All measured displacement data on fiber bundles were corrected accordingly.

The force applied to the sample is a superposition of the applied force, the force due to the length change of the bellow, the force due to heating induced length changes of the sample and the force resulting from dynamic pressure of the gas flow. The measured force has to be corrected for the force exerted by the bellow and the force due to the dynamic pressure of the gas flow. To correct the force exerted by the bellow a force measurement without sample was performed as a function of traverse position, i.e. expansion of the bellow. The force measured during the experiment was corrected accordingly. The effect of the gas flow was taken into account by applying the desired force at gas flow zero. Then the gas flow was chosen and the change of force was corrected to the original value.

Further details can be found in the specifications of the obtained patent [39].

2.2. Fiber material

The polyacrylonitrile precursor fiber used was a 6k tow produced by Bluestar (Grimsby, UK). Prior to carbonization the fibers were stabilized under oxidative atmosphere (synthetic air) in a separate experimental setup [40] that allows for precise control of mechanical tension and of heating rate in the temperature region below 300°C. Tows of 14cm length were stabilized at a constant force generating an initial stress of 2.5MPa. The temperature cycle was selected on basis of differential scanning calorimetry (DSC) measurements. The tows were heated to 150°C at a heating rate of 5K/min and subsequently to 250°C at 1.25K/min. This maximal temperature of 250°C was held for 20min. These stabilization parameters allow for subsequent carbonization within a wide parameter range.

Carbonization of the tows under defined tensile load was carried out using the experimental setup described in 2.1 and various final temperatures. The maximal final temperature was 1200°C. The

heating rate was set to 10K/min for all specimens, which represents a slow heating process in comparison to industrial carbon fiber production. For carbonization the fiber bundles were loaded by defined stresses between 0.5MPa and 4MPa. Carbonization was carried out under an atmosphere of Nitrogen 5.0 at a flow-rate of 250sccm.

Additionally, carbonization up to a maximal final temperature of 1600°C was performed without application of load. A furnace of type LORA 1800-32-600-1 (HTM Reetz GmbH) and a heating rate of 10K/min were used. Again, carbonization was performed under an atmosphere of Nitrogen 5.0 at a flow-rate of 250sccm.

2.3. Diagnostics

Synchronous Thermal Analysis (STA) was performed with a Netzsch STA 449 F3 Jupiter in the temperature range up to 1500°C, which allows simultaneous recording of Thermogravimetry (TG) and Differential Thermal Analysis (DTA). Starting material for the STA measurements were the stabilized precursor PAN fibers described above. About 60mg of chopped stabilized PAN fibers were placed in a ceramic crucible and heated under nitrogen atmosphere with a heating rate of 10K/min.

All carbonized fiber specimens carbonized in the setup presented in section 2.1 were investigated by microscopy, x-ray diffraction (XRD), and Raman diagnostics.

After embedding the carbonized tow in resin (Struers epofix) cross sections of the fiber specimen were prepared by grinding and polishing. Images of the fiber cross-sections were obtained by a digital light microscope (Keyence VHX-600). The software ImageJ [41] allows for analysis of the fiber cross-sections concerning area and effective diameter. The effective diameter is calculated from the measured area by assuming a circular shape. For this analysis the average of about 150 individual fibers was taken.

X-ray diffraction analysis was carried out using a Seifert XRD 3003 PTS diffractometer system with Cu K α ($\lambda=1.54\text{\AA}$) radiation. Wide-angle diffraction patterns were recorded in the range of 2θ between 10° and 40°. The fiber bundle was oriented perpendicular to the diffraction plane. Thus the 002-diffraction peak of graphitic carbon material is visible. Interlayer spacing and crystallite size L_c in c-direction (perpendicular to the graphene layers) were determined by the Bragg-Formula and the Scherrer-Equation with a shape factor of 0.89, respectively. The ratio of the area of the 002-diffraction peak and the area below the baseline of this peak gives a measure for the crystallinity of the fibers. Additionally, the angle χ was varied in the range between -70° and 70°, while the 2θ -position was set to the maximum of the 002-reflection. The full width at half maximum (FWHM) of this χ -scan represents a measure of the orientation of the crystallites. At lower values of FWHM the crystallites show a higher degree of orientation along the fiber axis.

Raman spectroscopy was performed at a Thermo Fisher Scientific DXR Raman microscope using a diode-pumped solid-state laser with a wavelength of 532nm. Spectra were recorded in the range from 800cm⁻¹ to 2000cm⁻¹. The D- and G-bands of graphite are found at about 1360cm⁻¹ and 1600cm⁻¹, respectively. The D- and G-band intensities are extracted from the areas of the respective peaks after baseline correction and peak fitting using pseudo-Voigt functions.

Single fiber tensile tests were performed by a ZwickiLine Z5.0 tensile testing machine (Zwick GmbH) using a 5N force cell. For all measurements of Young's modulus a gauge length of 35mm and a testing speed of 2mm/min were used. The gauge length for the measurement of tensile strength was 10mm

and the testing speed was 1mm/min. For each parameter 20 individual fibers were tested and the arithmetic mean value was obtained.

3. Results

3.1. Shrinkage of fibers during carbonization

To investigate the length change of stabilized PAN fibers and the influence of mechanical tensile load applied to the fibers during the carbonization treatment, stabilized PAN fibers were heated under inert atmosphere up to 1000°C at a heating rate of 10K/min using the experimental setup described in 2.1. Simultaneously, the length of the fibers was measured as function of temperature. The initial stress on the stabilized 6k tows was ranging from 0.5 to 3MPa. The initial stress was determined by measuring the average cross-sectional area of the stabilized fibers and adjusting the force generated by the tensile testing machine. This force is kept constant during the successive carbonization treatment. It should be emphasized that for the measurements shown the stress is not constant throughout carbonization, as the diameter of the fibers changes. We thus can only specify the *initial stress*.

Figure 3 shows the relative length changes of the tows as function of temperature for five different initial stresses (0.5MPa, 1MPa, 2MPa, 3MPa and 4MPa). Also, the corresponding rates of shrinkage are shown. In the temperature region of stabilization below 250°C no significant length changes are observed. Therefore, the length of each sample at 220°C (zero rate of length change) is used as reference point and calibrated to 100%. This way the different initial elongations due to the application of the different initial stresses are settled. The error bar indicated for the relative length data obtained at 0.5MPa is representative for all measurements.

Additionally, the length changes of fiber tows carbonized without application of load up to temperatures of 1000°C, 1200°C, 1400°C, and 1600°C are included in Figure 3. The length change of these fibers was determined by manual measurement of the bundle length after stabilization and after carbonization treatment.

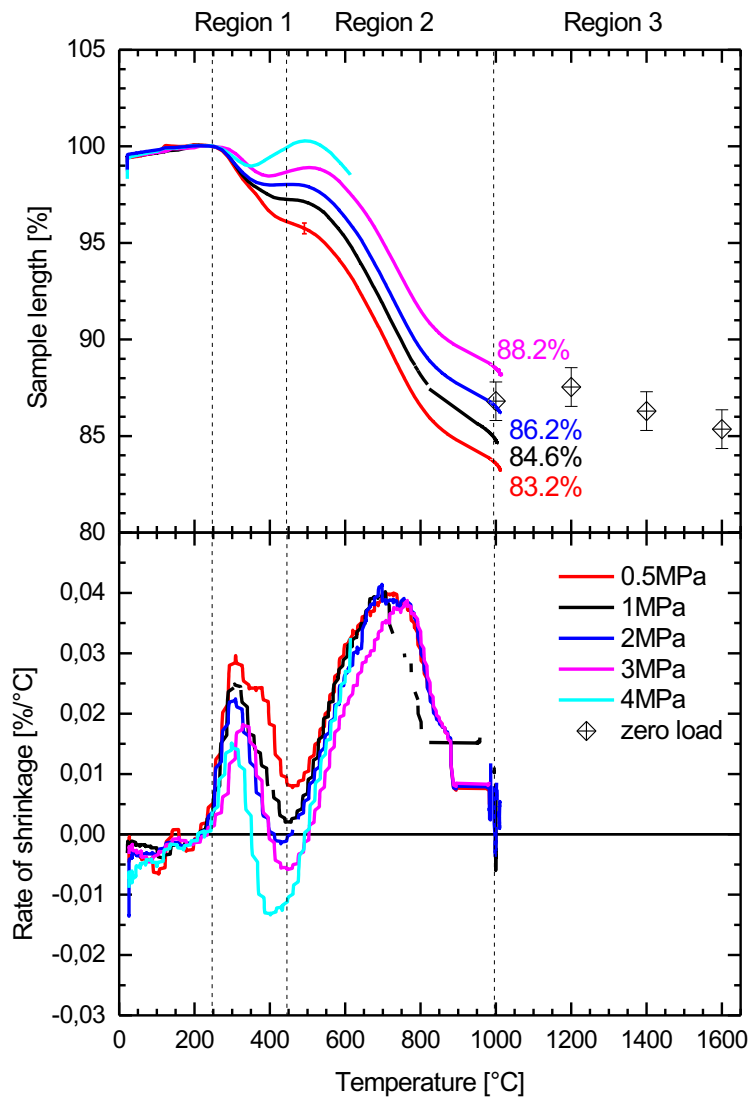


Figure 3: Length change and rate of shrinkage of tows during heat treatment for different initial stresses.

The behavior of length change of the fiber tows at temperatures above 250°C can be divided into three characteristic regions. The first region stretches from 250°C to 450°C, the second from 450°C to 1000°C and the last from 1000°C to the maximal temperature of 1600°C, as marked in Figure 3. The specified regions are described in the following.

Region 1: 250°C to 450°C

At a temperature of about 250°C the fibers start shrinking. The lower the mechanical stress, the higher the rate of shrinkage of the fibers. At about 300°C maximum rate of shrinkage is found, reaching 0.028%/°C for an initial stress of 0.5MPa and only 0.015%/°C for 4MPa. Above 300°C the rate of shrinkage decreases. At temperatures around 450°C, nearly constant sample lengths and a minimum in shrinkage rates near zero are reached. The minimal shrinkage rate and the

corresponding temperature depend on the applied tension. For 0.5MPa a shrinkage rate of 0.08%/°C is reached at 460°C. For 4MPa this minimum is already reached at 400°C and measures -0.013%/°C, which means that due to the higher load the fiber length even increases. For an initial tension of 2MPa the minimal rate at 430°C is around zero. Here, the fiber stops shrinking but still does not extend its length. In summary, at the boundary of Region 1 the shrinkage of the fibers is either minimal or even slight elongation is observed for high applied tensions, which is in good agreement with Refs. [38]. Also the observed influence of applied tensile load on the shrinkage behavior agrees well with reported data [16, 38].

Shrinkage in Region 1 is attributed to different effects. First, depending on the stabilization process, leftovers of the initial PAN material are likely to exist. This results in a continuation of stabilization reactions in this temperature region and the corresponding chemical shrinkage due to cyclization reactions [16, 38]. Secondly, high molecular weight material can be released, resulting from fragmentation of ladder-like molecules in uncyclized regions of the material [16, 38]. Finally, entropic shrinkage takes place. This kind of shrinkage especially depends on the applied tensile load, which can restrict relaxation effects and even extend coiled macromolecules [38].

Region 2: 450°C to 1000°C

In Region 2 the shrinkage of all fibers up to a temperature of about 730°C increases again, marked by a constantly increasing rate of shrinkage. This rate is almost independent of the applied tensile load and the same maximum rate of shrinkage of 0.039%/°C is reached for all applied loads. Fibers under an initial stress of 4MPa and higher (not shown in the figure) show tensile failure in this temperature region. For an initial stress of 4MPa failure occurred at 610°C. Above 730°C a decrease of the rate of shrinkage is observed, which is also independent of the applied initial stress and in good agreement with data from literature [16, 38].

Shrinkage in Region 2 is assumed to originate from crosslinking reactions between heterocyclic ladder-like molecules and/or larger heterocyclic structures, which result in the formation of graphite-like layers [38]. Mainly cross-linking along the fiber axis is assumed to be responsible for shrinkage in fiber direction. Our results indicate that this chemical process is not dependent on the applied load.

The relative residual length of the fibers at 1000°C, which represents the total length change over the complete temperature range up to 1000°C, ranges between 83.2% and 88.2% and increases with increasing applied initial stress. Thus, the higher the applied initial stress the lower the shrinkage, in agreement with Refs. [16, 38]. Realization of a higher residual length of our fibers by application of a higher load is not successful, as fiber breakage is induced. This is in contrast to residual lengths of more than 90%, which have been reported [16, 38, 42]. A correlation between the stabilization degree of the starting fibers and the amount of shrinkage during carbonization is described by Manocha et al. [16]. High stabilization degrees thus result in lower shrinkage during carbonization, i.e. higher residual length, which indicates, that the stabilized fibers used for our carbonization treatment reveal a relatively low degree of stabilization.

Region 3: 1000°C to 1600°C

The residual lengths of fibers carbonized without application of load up to maximal temperatures between 1000°C and 1600°C show no further development exceeding the margins of error. In average a value of (86.5±0.9) % is found. This saturation of shrinkage indicates a completion of the carbonization induced length changes. While the residual length agrees well with literature [42], we

expected slightly lower values based on our stress dependent measurements. Systematic differences between the manual length measurement of the fiber bundles carbonized without applied stress and the measurements using the universal testing machine are assumed to be the reason for this deviation.

In Region 3 further intermolecular cross-linking takes place. As the involved graphite-like planar structures are of high size and rigidity, movement is restricted, which prevents further shrinkage [38].

3.2. Cross section and volume of heat treated fibers

In addition to the analysis of shrinkage in fiber direction the change of fiber diameter during carbonization treatment was investigated. For that purpose, fiber specimens treated up to 400°C, 600°C, 750°C, 1000°C, 1200°C, 1400°C, and 1600°C were prepared. Figure 4 shows representative cross-sections of the stabilized fibers and of the fibers heat treated up to 750°C at an initial stress of 2MPa. A clear decrease of fiber diameter after additional heat treatment is observed.

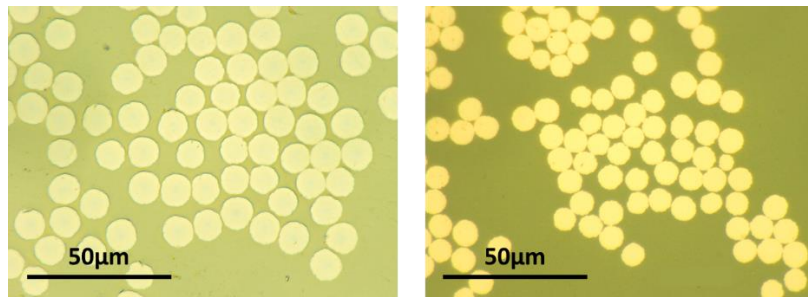


Figure 4: Micrographs of the cross-sections of the stabilized fiber (left) and the fibers treated to 750°C at 2MPa (right).

Figure 5 illustrates the evolution of fiber diameter as a function of heat treatment for different initial stresses. For comparison, also the diameters of the initial PAN precursor fiber and the stabilized fiber are shown. Both the absolute values of fiber diameter and the relative values, normalized to the diameter of the stabilized fiber, are shown. Figure 6 shows the change of fiber volume (calculated from fiber length and diameter) relative to the stabilized fiber as function of heat treatment temperature. In both figures, the temperature regions defined above are marked.

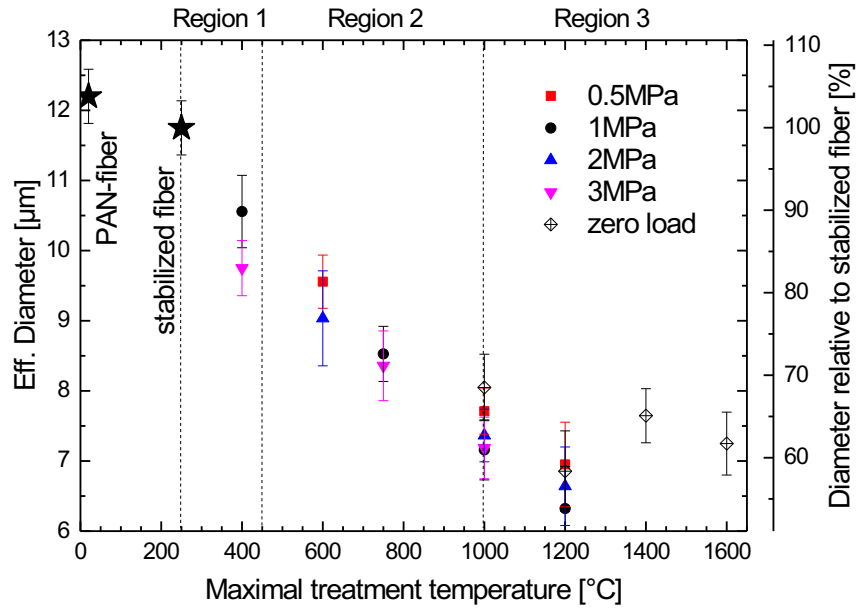


Figure 5: Absolute and relative fiber diameter as function of the maximal treatment temperature.

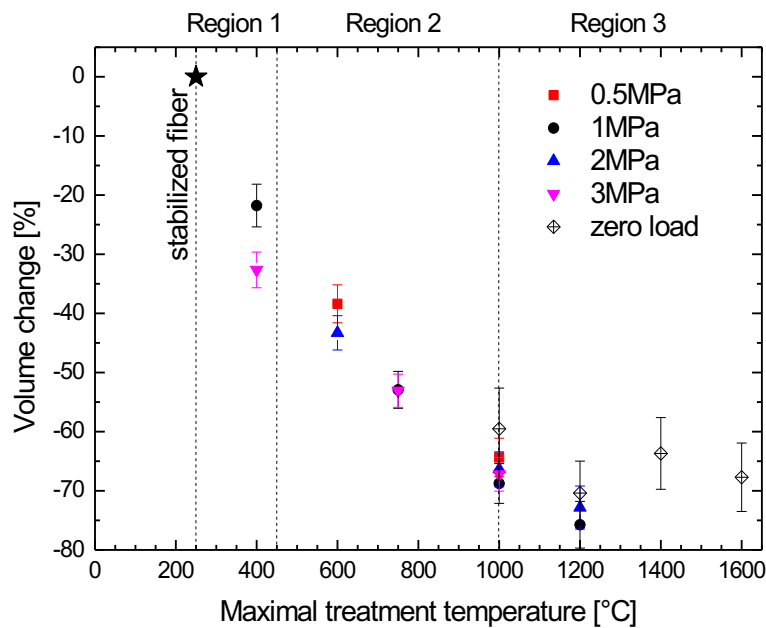


Figure 6: Relative change of fiber volume as function of the maximal treatment temperature.

During stabilization, the effective fiber diameter decreases from $12.2\mu\text{m}$ (PAN fiber) to $11.8\mu\text{m}$ (stabilized PAN fiber), i.e. by 3.3%, and is in good agreement with the reported values of $12\mu\text{m}$ [31] and of $11.5\mu\text{m}$ [43] respectively.

During heat treatment of the stabilized fibers up to a temperature of 450°C (Region 1) further decrease of fiber diameter of -10% to -17% is observed, but at a significantly higher rate. The reduction of diameter is significantly higher than shrinkage in fiber direction and therefore

dominates the fiber volume decrease. The decrease of diameter and volume in Region 1 is higher for high applied initial stress, i.e. applied stress hinders shrinkage in fiber direction but favors radial shrinkage. The chemical changes in Region 1, i.e. cyclization of remaining PAN, cross-linking of heterocyclic ladder-like molecules, release of high molecular weight material and entropic shrinkage [12, 16, 38], thus have significantly higher impact on the radial dimensions of the fiber. The influence of tensile load on the diameter points to the impact of entropic shrinkage.

For higher heat treatment temperatures (Region 2) fiber diameter and volume decrease further, but at a lower rate. Similar data – although without variation of tension – have been reported [44]. Still, radial shrinkage is significantly stronger than shrinkage in fiber direction. The dominant chemical changes in this temperature region, i.e. cross-linking of heterocyclic ladder-like molecules and/or heterocyclic planar molecules and the starting stacking of these layers to turbostratic carbon [12, 13, 38], take place mainly in direction perpendicular to the fiber axis. Consequently, they reveal a high impact on radial dimensions. Differences in fiber diameter and volume due to different applied stresses vanish throughout heat treatment.

During heat treatment from 1000°C to 1600°C the diameter does not change beyond the margins of error. An average diameter of 7.2 μm is reached. Consequently, the volume remains fairly constant in this temperature region. This saturation of the fiber dimensions indicates the completion of the carbonization of the fibers. Again, the restricted movement of the developing graphite-like planar structures is assumed to be the reason [38].

Over the whole temperature range the radial shrinkage exceeds the length change by a factor of more than two. The total volume change amounts to -65% to -70%.

3.3. Thermal analysis

Mass changes and heat flow during carbonization of stabilized PAN fibers, which provide information about ongoing chemical reactions, were investigated by STA. Figure 7 shows the TG and DTA curves. The observed curve shape can be classified according to the three characteristic temperature regions defined above.

In the temperature range below 250°C a slight mass loss of 2% is observed, probably due to the loss of water.

In Region 1 a significant mass loss is observed, as the residual mass drops from 98% to 80% of the initial mass. This drop also has been reported by Refs. [16, 24, 45]. At 380°C the rate of mass loss (DTG, *differential thermogravimetry*) reaches its extremal value. In the same temperature region, the heat flow reaches a slight maximum, indicating a specific exothermic chemical reaction taking place. The mass loss in Region 1 is attributed mainly to dehydrogenation. Water is released, resulting from condensation reactions of hydroxy groups or hydroxy and carbonyl groups of ladder-like polymers [12, 13, 16].

Region 2 is characterized by a further mass loss but at a smaller rate, which is minimal around 700°C. For temperatures between 700°C and 1000°C further mass loss is observed at an increasing rate. Here denitrogenation is assumed, resulting from coalescence of planar heterocyclic structures [12, 13, 42]. The rate of mass loss shows a local extremal value at around 1000°C. At 1000°C a residual mass of 59.6% of the initial mass remains, which agrees with reported data [25]. The DTA signal shows two maxima at temperatures of about 640°C and 900°C, pointing to further specific exothermic reactions.

In Region 3 mass loss approaches zero and the DTA signal decreases rapidly. At the maximal temperature of 1500°C, the residual mass measures 52.1%. This finding agrees with a reported mass yield of >50% compared to the original precursor [10].

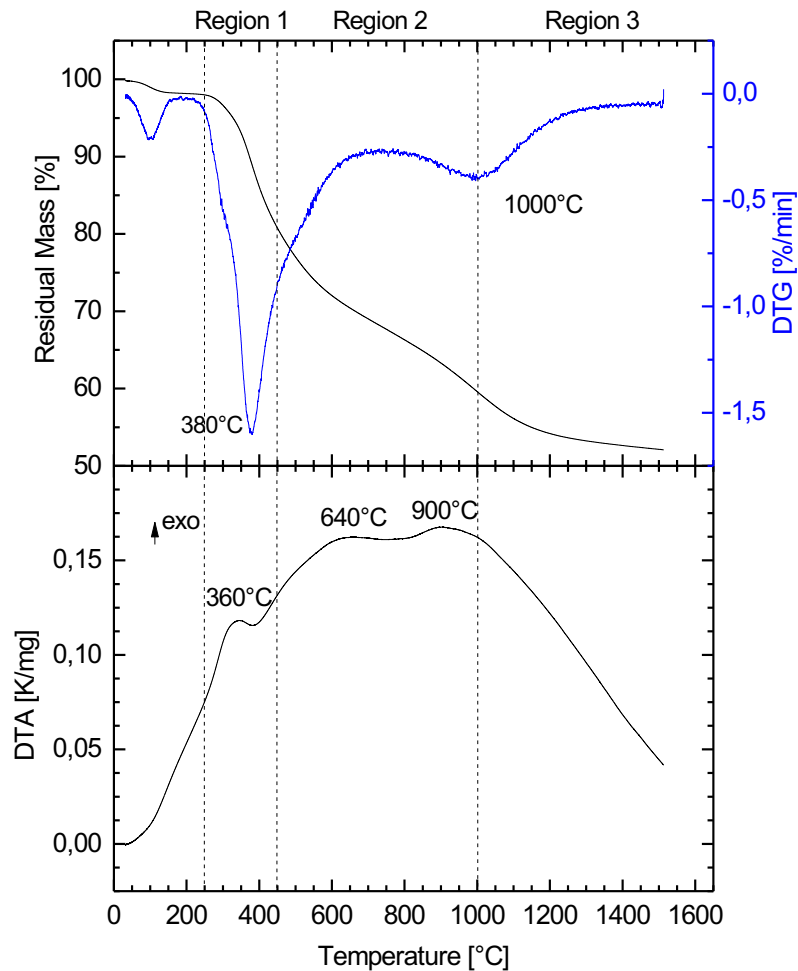


Figure 7: STA measurements of the stabilized PAN fiber material: Thermogravimetry (residual mass and its derivative) and Differential Thermal Analysis.

3.4. X-ray analysis of carbonized fibers

Next, the evolution of the crystalline microstructure of the fibers during the carbonization process is addressed by XRD. Figure 8 shows the diffraction patterns of the fibers heat treated to different maximal temperatures between 250°C and 1200°C under a defined tensile stress of 0.5MPa and the pattern of the fibers carbonized to 1600°C without mechanical load.

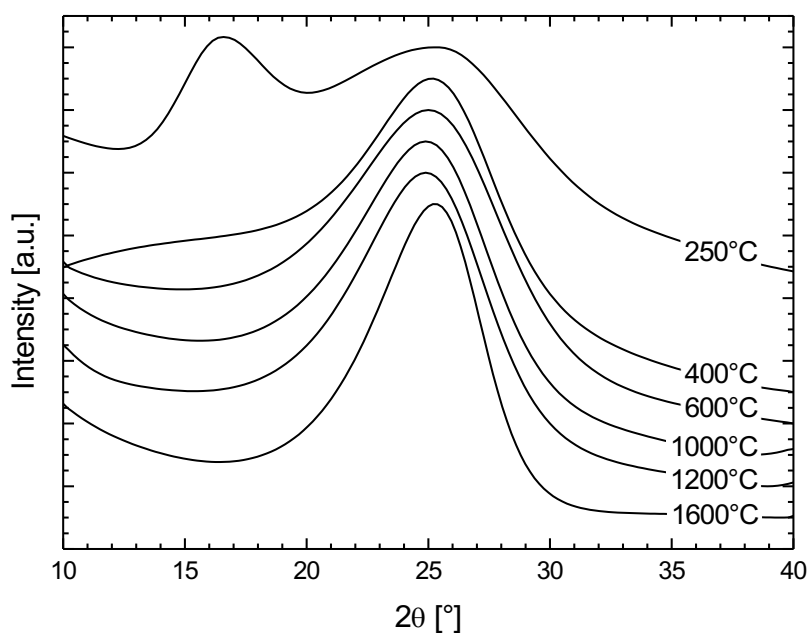


Figure 8: XRD diffraction patterns of fibers heat treated up to different maximal temperatures (0,5MPa).

For the stabilized fiber heated up to 250°C a broad peak at about 25° is observed, which is attributed to layered structures of ladder-like heterocyclic polymers [46]. Additionally, a diffraction peak at $2\theta=17^\circ$ is found, originating from the initial PAN structure [17, 22, 45, 47]. The measurements thus demonstrate that the fiber has not been stabilized completely, as a significant part still shows PAN structure. This is a common observation after stabilization treatment [17, 45, 48]. The results also agree with the shrinkage measurements shown above, indicating a relatively low residual length after carbonization treatment due to a low degree of stabilization of the starting fibers.

After heat treatment up to 400°C the peak at $\theta=17^\circ$, attributed to the PAN-structure, has almost vanished while the peak at 25° has sharpened significantly, in agreement with existing data [24]. Thus, during heat treatment in the temperature range of Region 1 unreacted PAN completes cyclization. Additionally, cross-linking of heterocyclic ladder-like polymers to planar heterocyclic planes and improved stacking of the layers is assumed to take place, resulting in a sharpening of the corresponding reflex at 25°. Its position coincides with that of the (002) reflex of graphite, indicating the formation of a pre-stage material of turbostratic graphite.

With ongoing heat treatment, i.e. in Regions 2 and 3, the peak at $2\theta=25^\circ$ increases in intensity and becomes sharper, which results from the developing graphite-like turbostratic structure formed by coalescence of heterocyclic ring structures and the removal of heteroatoms [17, 24]. The formation of aromatic carbon basal planes is supposed to start at 550°C-600°C [17]. For heat treatment up to 1600°C the peak maximum shifts to higher angles, indicating a decrease of interlayer spacing.

The evaluation of the peak shape of the XRD peak at $2\theta=25^\circ$ reveals the crystallite parameters of the stacked heterocyclic polymers (< 600°C) developing to graphite-like turbostratic carbon (> 600°C). As we deal with the (002)-reflection of graphite, we measure the properties perpendicular to the layers (c-direction). Figure 9 shows the corresponding crystallite size, the FWHM of the χ -scan (a measure of the orientation of the crystallites), the interlayer spacing and the crystallinity as function of the maximal heat treatment temperature.

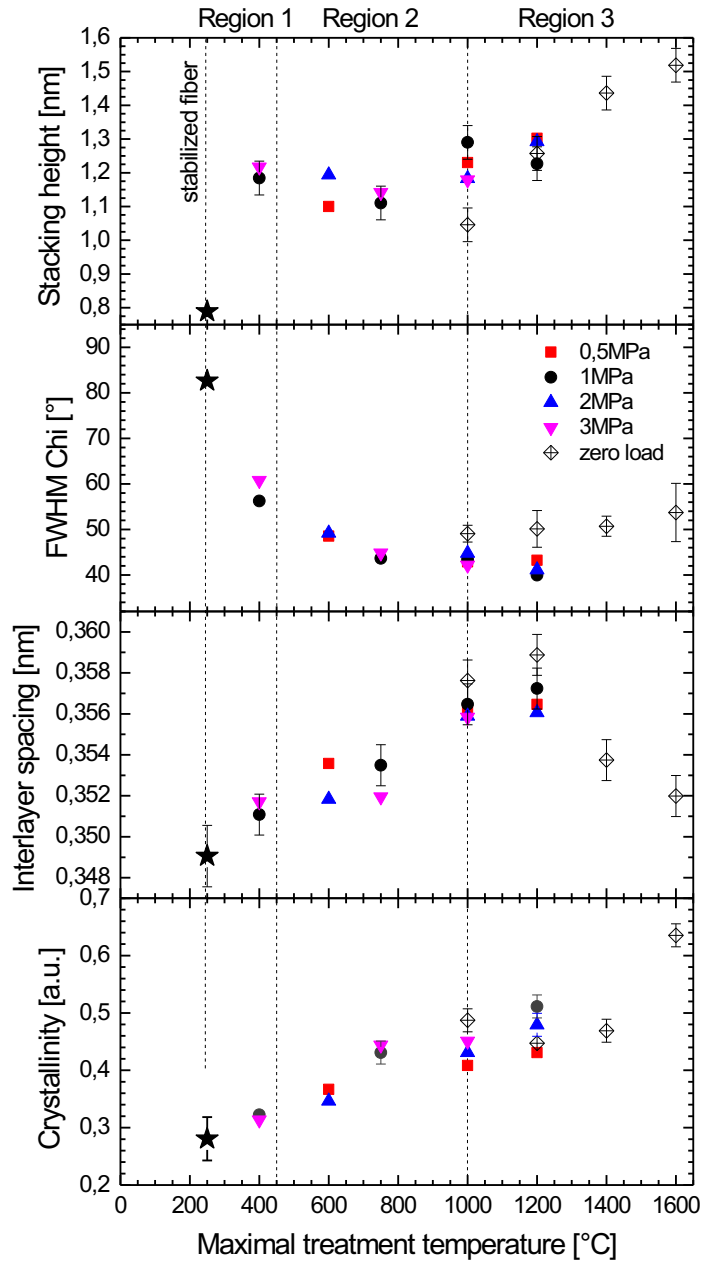


Figure 9: Crystallite size, FWHM of χ -scan, interlayer spacing, and crystallinity determined by XRD measurements as function of maximal heat treatment temperature.

The specimens treated up to a temperature of 400°C (Region 1) show a significant growth of the stacking height of the layer structures and a moderate increase of crystallinity. The increasing crystallinity can be due to either growth of already existing crystallites or the formation of new crystallites or both. The FWHM of the χ -scan decreases clearly, indicating an increase of orientation of the crystallites along the fiber axis. The results are in good agreement with reported data [44]. Interlayer spacing is rising in this region, probably due to the pronounced reordering of the material in this temperature range. Anyway, due to the broadness of the peaks, this change does not exceed the margins of error.

In Region 2, where the heterocyclic layer structure becomes more graphite-like [17], further increase of the crystallinity and decrease of the FWHM of the χ -scan is found, while the stacking height does not change significantly. The increase of interlayer spacing affirms the findings of others [17].

During heat treatment up to 1600°C (Region 3), the FWHM of the χ -scan remains constant within the margins of error. Saturation of the crystallite orientation seems to be achieved, possibly because the increasing lateral extension of the graphite-like structures hinders movement. Crystallite size and crystallinity increase significantly, which is typical for this temperature region [14, 23, 44]. Interlayer spacing takes a turnaround at 1200°C, where a maximal value of 0.359nm is reached. Above this temperature the well-described decrease of interlayer spacing is observed [12, 14, 23]. It results in a spacing of 0.352nm at 1600°C, which is characteristic for PAN-based carbon fibers [12, 49, 50]. Also crystallinity (0.64) and stacking height (1.52nm) at 1600°C match the values of commercial carbon fibers [23, 49, 51]. Thus, up to the maximal heat treatment temperature of 1600°C the turbostratic lattice gradually improves its stacking order.

The applied stress is found to play a minor role regarding the crystalline properties in Regions 1 and 2. Anyway, in Region 3 slight differences in crystallinity are found, showing increasing crystallinity in the order of tensile stress 0.5MPa < 2MPa < 1MPa. As no changes in crystallite size are observed, a stress induced formation of new crystallites seems to occur. This has not been reported so far.

3.5. Raman spectroscopy of carbonized fibers

Figure 10 shows the Raman spectra of the fibers treated to different maximal temperatures. The G-band at about 1360cm⁻¹ is attributed to the E_{2g}-mode of graphite. The D-band at about 1600cm⁻¹ is assigned to the A_{1g}-mode that is forbidden in perfect graphite and becomes Raman-active due to perturbations of the crystalline order [52, 53]. All intensities are normalized to the maximum of the D-band. The G-band intensity increases with increasing carbonization temperature until at 750°C it reaches a peak height similar to the D-band. Above 750°C only minor changes are observed. For different stresses applied during heat treatment no significant differences between the spectra are found (not shown in the figure).

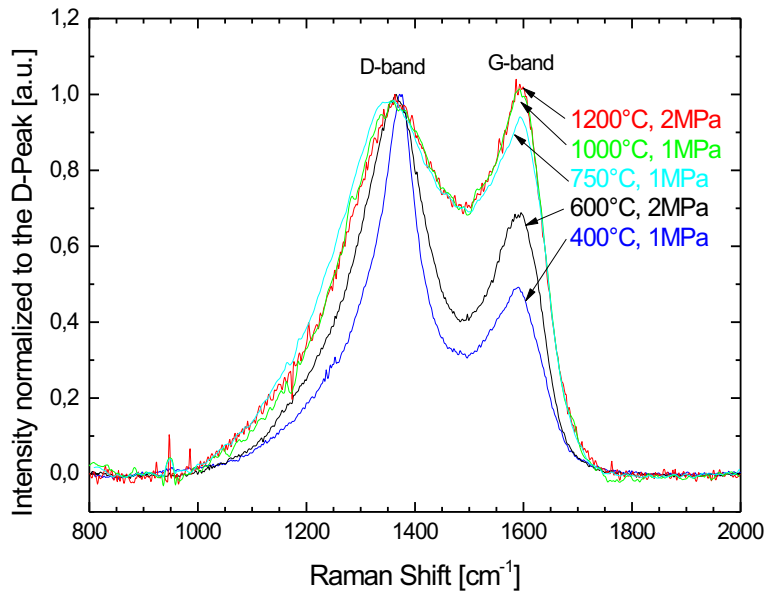


Figure 10: Raman spectra of fibers carbonized to different maximal treatment temperatures (different colors) at an applied initial stress of 1MPa or 2MPa. The intensities are normalized to the maximum of the D-Peak.

Figure 11 shows the ratio of the D- and G-band-intensities determined as described above. The ratio of the intensities of D- and G-band is a measure of the degree of amorphous carbon material [54]. It is reported to be inversely proportional to the lateral crystallite size L_a of the turbostratic graphitic crystallites (for $L_a > 2\text{nm}$), which is the size of a graphene layer [55–57]. However, this empirical correlation must be used with caution. While the D-band generally indicates the existence of six-fold aromatic rings, the G-Band, which is characteristic for graphite, not only occurs in graphitic materials but also due to any in-plane bond-stretching of two sp^2 -carbons [54]. Thus, for the low temperature range in Region 1, where no larger graphite-like regions are expected, the intensity ratio is no reliable indicator for crystallite size and will not be discussed in the following.

In the high temperature range, i.e. in Region 2 and Region 3, a continuous decrease of the $I(D)/I(G)$ ratio as function of maximal treatment temperature is found, which indicates an increase of the lateral extension of the graphite-like crystallites. The value of 2.46 achieved at the highest heat treatment temperature of 1600°C is in very good agreement with literature data on commercial carbon fibers [49].

Over the whole temperature range up to 1600°C, the applied tensile stress shows no significant impact on D/G. The lateral crystal growth seems to be independent of the applied load, which has not been shown in literature so far.

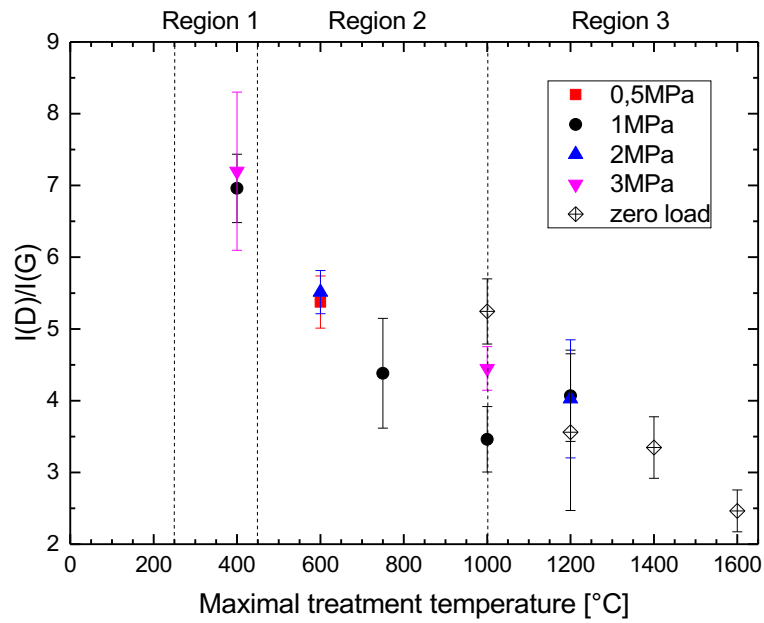


Figure 11: Ratio of the intensities of D- and G-band in Raman spectra of heat treated fibers.

3.6. Mechanical properties

During heat treatment the fibers experience a drastic change in mechanical behavior. Figure 12 shows the stress-strain-curves of the stabilized fibers as well as the fibers heated to different maximal temperatures under an applied stress of 0.5MPa.

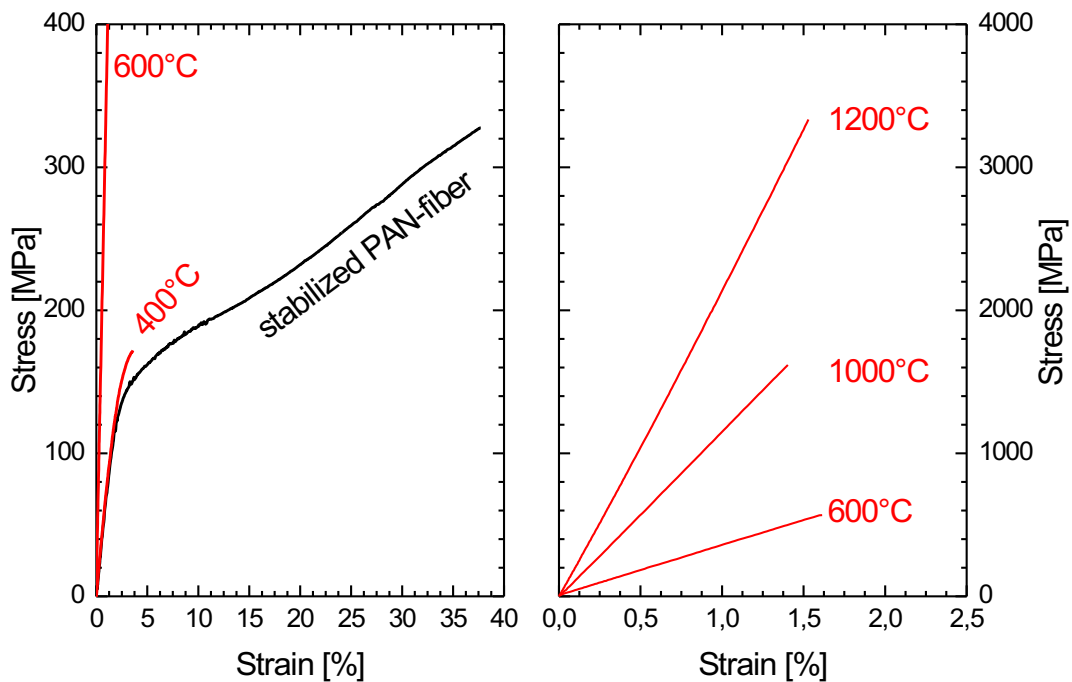


Figure 12: Stress-strain-curves of the stabilized fiber and the fibers after heat treatment to different maximal temperatures under a stress of 0.5MPa.

The stabilized fiber shows a linear elastic behavior for strains below 2%. At higher strains plastic deformation takes place, indicated by a deviation of the curve from linear behavior. This behavior is characteristic for semi crystalline polymers like PAN. The stress-strain-curve underlines the XRD observations that after stabilization a significant rest of unreacted PAN remains, resulting in the polymer-typical failure behavior of the fibers.

After heat treatment to 400°C for strains below 2% a similar linear elastic behavior is observed. For higher strains, much smaller deviation from linear behavior takes place until fiber breakage, pointing to an occurring embrittlement. A significantly reduced tensile strength is found. The observations hint at the completion of stabilization of remaining parts of PAN, since increased stabilization degrees result in reduced tensile strength [43] and an embrittlement of the fibers. Good agreement with the XRD results can be stated, which indicate nearly completed stabilization at this temperature. Heat treatment of the fibers to 600°C results in further changes of the stress-strain-curve. Only linear elastic behavior up to fiber breakage at significantly higher stress values is found, indicating a brittle material with strongly increased modulus and tensile strength. A further increase of temperature leads to a pronounced increase of strength and modulus. The resulting mechanical parameters as function of heat treatment temperature for different applied stresses are depicted in Figure 13.

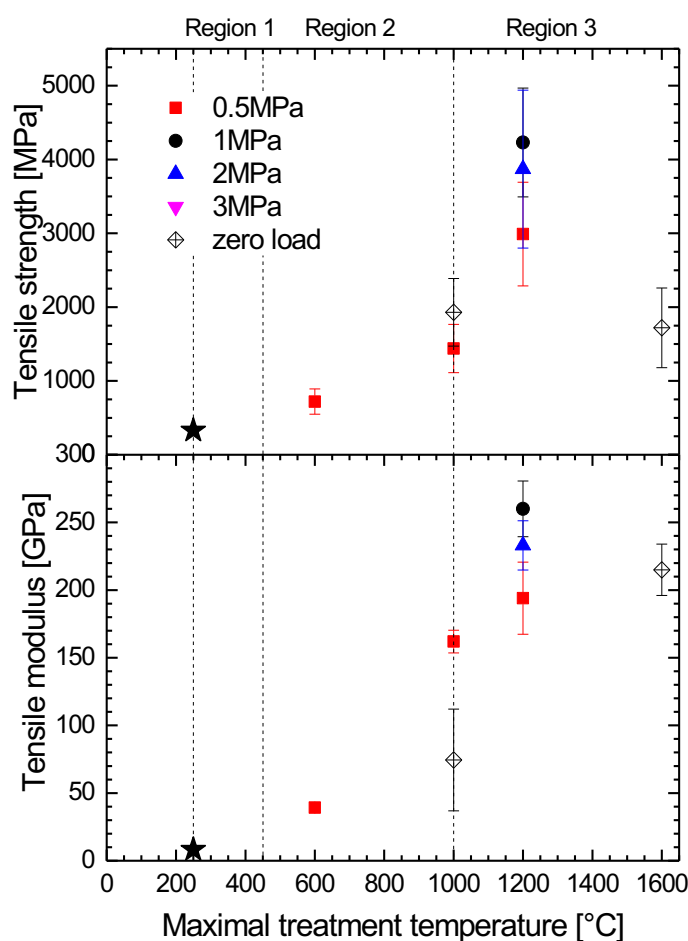


Figure 13: Mechanical properties of fiber samples heat treated under different tensile load to different maximal temperatures.

An increasing heat treatment temperature is reported to lead to higher strength and modulus values [12, 24, 42, 44]. Our fibers confirm this trend and show tensile moduli up to 260GPa and strengths up to 4230MPa after carbonization to 1200°C, i.e. their mechanical properties are similar to that of commercial carbon fibers [49, 58, 59]. The heat induced development of a turbostratic graphitic structure is assumed to be the reason for this continuous improvement of mechanical properties. The results demonstrate the ability of our experimental setup to perform reliable carbonization heat treatment of PAN-based fibers. Also, the stabilization treatment of our fibers is well chosen.

The mechanical properties of fibers carbonized to 1200°C show a dependence on the tensile stress. By trend, modulus and strength are highest for a stress of 1MPa applied during heat treatment. A stress of 0.5MPa results in the lowest mechanical properties whereas 2MPa lead to intermediate values. The same stress-dependence was observed for the crystallinity, which suggests a correlation between these two physical properties. Stress induced crystallite formation thus results in an improvement of tensile properties of the fibers.

Köhler et al. report strength and modulus values of carbon fibers based on the same precursor material and carbonized to a similar maximal temperature [31]. The reported values are close to our values observed after carbonization under an applied stress of 0.5MPa. After carbonization under a stress 1MPa our fibers show even higher mechanical properties, which underline the possibility of a significant optimization of mechanical parameters by defined application of stress.

The absence of tensile stress during carbonization significantly reduces the fiber modulus, in agreement with data from literature [16]. Our data shows no clear influence of load on the fiber strength at 1000°C, but a clearly lower strength value at 1600°C for carbonization without applied load.

4. Conclusion

A newly developed experimental setup was utilized to investigate the carbonization of stabilized PAN fiber bundles. The setup allows to carbonize fiber specimen with a defined temperature program (used parameters: maximal temperature 1200°C, heating rate 10K/min) and a defined mechanical load applied to the fiber bundle. The carbonization induced shrinkage of the specimen was measured online during heat treatment as a function of temperature. For high accuracy the fiber bundles are clamped within the hot section of the furnace. After heat treatment the fiber specimens were investigated as to diameter, mechanical properties, and crystalline properties.

Three characteristic temperature regions for the carbonization process were identified.

Between 250°C and 450°C the fibers still contain a PAN-like polymeric phase which experiences ongoing stabilization reactions. The stress-strain curve hints at a polymer-like ductile failure behavior. The cross-linking of existing heterocyclic ladder-like molecules results in the growth of stacked, heterocyclic planar structures. The orientation of these structures along the fiber axis strongly increases. Between 450°C and 1000°C these crystallites develop to graphite-like turbostratic carbon. They grow in lateral dimension and align further along the fiber axis while crystallinity increases. The material has become brittle. Above 1000°C further increase of stacking height and crystallinity occurs. Mass-loss and shrinkage approach zero. The interlayer distance decreases as the graphite-like structure is improved. Mechanical properties approach the values of commercial carbon fibers.

Application of a tensile stress during carbonization treatment of the fibers revealed the following trends.

First, fiber dimensions are influenced by tensile stress at temperatures between 250°C and 450°C where the material is ductile. Tensile stress hinders shrinkage in fiber direction and furthers axial shrinkage.

Secondly, at temperatures above 1000°C, crystalline parameters and mechanical properties of the resulting carbon fibers depend on the applied stress. At 1200°C strength, modulus and crystallinity are highest for an applied tension of 1MPa. Carbonization without tensile stress results in significantly lower mechanical properties.

The results show the impact of heat treatment temperature and stress applied during carbonization on the carbon fiber properties. They demonstrate the possibility of tailoring fiber mechanical properties by adjusting heat treatment temperature and applied tensile stress.

Acknowledgement

We thank Professor Dr. Dirk Volkmer (Chair of Solid State Chemistry, University of Augsburg) for the possibility to perform Raman measurements.

References

- [1] Balasubramanian M, Jain MK, Bhattacharya S. K., Abhiraman AS. Conversion of acrylonitrile-based precursors to carbon fibres: Part 3 Thermooxidative stabilization and continuous, low temperature carbonization. *Journal of Materials Science* 1987; 22: 3864–72.
- [2] Deurbergue A, Oberlin A. Stabilization and carbonization of pan-based carbon fibers as related to mechanical properties. *Carbon* 1991; 29(4–5): 621–8. doi:10.1016/0008-6223(91)90129-7.
- [3] Edie DD. The effect of processing on the structure and properties of carbon fibers. *Carbon* 1998; 36(4): 345–62. doi:10.1016/S0008-6223(97)00185-1.
- [4] Newcomb BA. Processing, structure, and properties of carbon fibers. *Composites Part A: Applied Science and Manufacturing* 2016; 91: 262–82. doi:10.1016/j.compositesa.2016.10.018.
- [5] Oberlin A. Carbonization and graphitization. *Carbon* 1984; 22(6): 521–41. doi:10.1016/0008-6223(84)90086-1.
- [6] S. Chand. Review Carbon fibers for composites. *Journal of Materials Science* 2000; 35: 1303–13.
- [7] Watt W. Carbon work at the royal aircraft establishment. *Carbon* 1972; 10(2): 121–43. doi:10.1016/0008-6223(72)90036-X.
- [8] Bajaj P, Roopanwal AK. Thermal Stabilization of Acrylic Precursors for the Production of Carbon Fibers: An Overview. *Journal of Macromolecular Science, Part C: Polymer Reviews* 1997; 37(1): 97–147. doi:10.1080/15321799708014734.
- [9] Fitzer E, Frohs W, Heine M. Optimization of stabilization and carbonization treatment of PAN fibres and structural characterization of the resulting carbon fibres. *Carbon* 1986; 24(4): 387–95. doi:10.1016/0008-6223(86)90257-5.
- [10] Rahaman MSA, Ismail AF, Mustafa A. A review of heat treatment on polyacrylonitrile fiber. *Polymer Degradation and Stability* 2007; 92(8): 1421–32. doi:10.1016/j.polymdegradstab.2007.03.023.
- [11] Ruhland K, Frenzel R, Horny R, Nizamutdinova A, van Wüllen L, Moosburger-Will J et al. Investigation of the chemical changes during thermal treatment of polyacrylonitrile and 15 N-labelled polyacrylonitrile by means of in-situ FTIR and 15 N NMR spectroscopy. *Polymer Degradation and Stability* 2017; 146: 298–316. doi:10.1016/j.polymdegradstab.2017.10.018.
- [12] Frank E, Steudle LM, Ingildeev D, Spörl JM, Buchmeiser MR. Carbon Fibers: Precursor Systems, Processing, Structure, and Properties. *Angew. Chem. Int. Ed.* 2014; 53(21): 5262–98. doi:10.1002/anie.201306129.
- [13] Goodhew PJ, Clarke AJ, Bailey JE. A review of the fabrication and properties of carbon fibres. *Materials Science and Engineering* 1975; 17(1): 3–30. doi:10.1016/0025-5416(75)90026-9.
- [14] Jain MK, Abhiraman AS. Conversion of acrylonitrile-based precursor fibres to carbon fibres. *Journal of Materials Science* 1987; 22(1): 278–300. doi:10.1007/BF01160584.
- [15] Johnson JW, Marjoram JR, Rose PG. Stress Graphitization of Polyacrylonitrile Based Carbon Fibre. *Nature* 1969; 221(5178): 357–8. doi:10.1038/221357b0.
- [16] Manocha LM, Bahl OP, Jain GC. Length changes in PAN fibers during their pyrolysis to carbon fibers. *Angew. Makromol. Chemie* 1978; 67(1): 11–29. doi:10.1002/apmc.1978.050670102.
- [17] Jing M, Wang C-g, Wang Q, Bai Y-j, Zhu B. Chemical structure evolution and mechanism during pre-carbonization of PAN-based stabilized fiber in the temperature range of 350–600 °C. *Polymer Degradation and Stability* 2007; 92(9): 1737–42. doi:10.1016/j.polymdegradstab.2007.05.020.
- [18] Standage AE, Matkowsky R. Structure of Oxidized Polyacrylonitrile. *Nature* 1969; 224(5220): 688–9. doi:10.1038/224688a0.
- [19] Wang Y, Xu L, Wang M, Pang W, Ge X. Structural Identification of Polyacrylonitrile during Thermal Treatment by Selective 13 C Labeling and Solid-State 13 C NMR Spectroscopy. *Macromolecules* 2014; 47(12): 3901–8. doi:10.1021/ma500727n.
- [20] Watt W, Johnson W. Mechanism of oxidisation of polyacrylonitrile fibres. *Nature* 1975; 257: 210–2. doi:10.1038/257210a0.
- [21] Watt W. Nitrogen Evolution during the Pyrolysis of Polyacrylonitrile. *Nat Phys Sci* 1972; 236(62): 10–1. doi:10.1038/physci236010a0.

- [22] Mathur RB, Bahl OP, Mittal J, Nagpal KC. Structure of thermally stabilized PAN fibers. *Carbon* 1991; 29(7): 1059–61. doi:10.1016/0008-6223(91)90189-P.
- [23] Takaku A, Shioya M. X-ray measurements and the structure of polyacrylonitrile- and pitch-based carbon fibres. *Journal of Materials Science* 1990; 25(11): 4873–9. doi:10.1007/BF01129955.
- [24] Lee S. Structural Evolution of Polyacrylonitrile Fibers in Stabilization and Carbonization. *ACES* 2012; 02(02): 275–82. doi:10.4236/aces.2012.22032.
- [25] Mathur RB, Dhama TL, Bahl OP. Shrinkage behaviour of modified PAN precursors—Its influence on the properties of resulting carbon fibre. *Polymer Degradation and Stability* 1986; 14(2): 179–87. doi:10.1016/0141-3910(86)90016-9.
- [26] Tse-Hao K, Tzy-Chin D, Jeng-An P, Ming-Fong L. The characterization of PAN-based carbon fibers developed by two-stage continuous carbonization. *Carbon* 1993; 31(5): 765–71. doi:10.1016/0008-6223(93)90013-Z.
- [27] Tsai J-S. Coefficient variation of the mechanical properties of carbon fiber during carbonization. *Journal of Polymer Research* 1994(1): 399.
- [28] Tsai J-S. Tension effects on the properties of oxidized polyacrylonitrile and carbon fibers during continuous oxidation. *Polymer Engineering and Science* 1995; 35(16): 1313–6. doi:10.1002/pen.760351607.
- [29] Tsai J-S. Tension of carbonization for carbon fiber. *Polymer Engineering and Science* 1994; 34(19): 1480–4. doi:10.1002/pen.760341907.
- [30] Tsai J-S. Optimization of carbon fibre production using the Taguchi method. *Journal of Materials Science* 1995; 30: 2019–22. doi:10.1007/BF00353027.
- [31] Köhler T, Pursche F, Burscheidt P, Seide G, Gries T. Optimization of process parameters during carbonization for improved carbon fibre strength. *IOP Conf. Ser.: Mater. Sci. Eng.* 2017; 254: 42018. doi:10.1088/1757-899X/254/4/042018.
- [32] Isaac DH, Ozbek S. Manufacture of High Performance Carbon Fibers from Precursors of Various Diameters. *Materials and Manufacturing Processes* 1994; 9(5): 975–98. doi:10.1080/10426919408934964.
- [33] Kleinhans H, Salmén L. Development of lignin carbon fibers: Evaluation of the carbonization process. *Journal of Applied Polymer Science* 2016; 133(38). doi:10.1002/app.43965.
- [34] Ozbek S, Isaac DH. Carbon Fiber Processing: Effects of Hot Stretching on Mechanical Properties. *Materials and Manufacturing Processes* 1994; 9(2): 199–219. doi:10.1080/10426919408934899.
- [35] Rennhofer H, Puchegger S, Pabisch S, Rentenberger C, Li C, Siegel S et al. The structural evolution of multi-layer graphene stacks in carbon fibers under load at high temperature – A synchrotron radiation study. *Carbon* 2014; 80: 373–81. doi:10.1016/j.carbon.2014.08.076.
- [36] Sauder C, Lamon J, Pailler R. The tensile behavior of carbon fibers at high temperatures up to 2400 °C. *Carbon* 2004; 42(4): 715–25. doi:10.1016/j.carbon.2003.11.020.
- [37] Younes A, Sankaran V, Seidel A, Cherif C. Study of tensile behavior for high-performance fiber materials under high-temperature loads. *Textile Research Journal* 2014; 84(17): 1867–80. doi:10.1177/0040517513499434.
- [38] Wu Z, Pan D, Fan X, Qian B. Thermal shrinkage behavior of preoxidized polyacrylonitrile fibers during carbonization. *Journal of Applied Polymer Science* 1987; 33(8): 2877–84. doi:10.1002/app.1987.070330821.
- [39] Gutmann P, Horny R, Sause M, Horn S, Moosburger-Will J. Vorrichtung und Verfahren zur Hochtemperaturprüfung von Werkstoffproben; German Patent Nr. 10 2016 124 085 (2018).
- [40] Frenzel R. Strukturelle und chemische Veränderung von Polyacrylnitril und Polyacrylnitrilfasern während der thermischen Behandlung. Dissertation. Universität Augsburg; 2016.
- [41] Rasband WS. ImageJ. Bethesda, Maryland, USA: U. S. National Institutes of Health; 1997-2016.
- [42] Mittal J, Konno H, Inagaki M, Bahl OP. Denitrogenation behavior and tensile strength increase during carbonization of stabilized pan fibers. *Carbon* 1998; 36(9): 1327–30. doi:10.1016/S0008-6223(98)00113-4.
- [43] Hameed N, Sharp J, Nunna S, Creighton C, Magniez K, Jyotishkumar P et al. Structural transformation of polyacrylonitrile fibers during stabilization and low temperature carbonization. *Polymer Degradation and Stability* 2016; 128: 39–45. doi:10.1016/j.polymdegradstab.2016.02.029.
- [44] Liu J, Wang P. H., Li R. Y. Continuous carbonization of polyacrylonitrile-based oxidized fibers: Aspects on mechanical properties and morphological structure. *Journal of Applied Polymer Science* 1994; 52(945-950). doi:10.1002/app.1994.070520712.
- [45] Yu M, Xu Y, Wang C, Zhu B, Wang Y, Hu X et al. Structure and property relations between the polyacrylonitrile-based prestabilized fibers and the partially carbonized fibers. *Journal of Applied Polymer Science* 2012; 124: 5172-5179. doi:10.1002/app.33810.

- [46] Ko T-H, Ting H-Y, Lin C-H, Chen J-C. The microstructure of stabilized fibers. *Journal of Applied Polymer Science* 1988; 35(4): 863–74. doi:10.1002/app.1988.070350402.
- [47] Lindenmeyer PH, Hosemann R. Application of the Theory of Paracrystals to the Crystal Structure Analysis of Polyacrylonitrile. *J. Appl. Phys.* 1963; 34(1): 42–5. doi:10.1063/1.1729086.
- [48] He D-X, Wang C-g, Bai Y-j, Lun N, Zhu B, Wang Y-X. Microstructural evolution during thermal stabilization of PAN fibers. *Journal of Materials Science* 2007; 42(17): 7402–7. doi:10.1007/s10853-007-1838-9.
- [49] Chae HG, Newcomb BA, Gulgunje PV, Liu Y, Gupta KK, Kamath MG et al. High strength and high modulus carbon fibers. *Carbon* 2015; 93: 81–7. doi:10.1016/j.carbon.2015.05.016.
- [50] Huang X. Fabrication and Properties of Carbon Fibers. *Materials* 2009; 2(4): 2369–403. doi:10.3390/ma2042369.
- [51] Tanaka F, Okabe T. 1.4 Historical Review of Processing, Microstructures, and Mechanical Properties of PAN-Based Carbon Fibers. In: *Comprehensive Composite Materials II*: Elsevier; 2018, p. 66–85.
- [52] Cuesta A, Dhamelincourt P, Laureyns J, Martínez-Alonso A, Tascón JMD. Comparative performance of X-ray diffraction and Raman microprobe techniques for the study of carbon materials. *J. Mater. Chem.* 1998; 8(12): 2875–9. doi:10.1039/a805841e.
- [53] Sato K, Saito R, Oyama Y, Jiang J, Cañçado LG, Pimenta MA et al. D-band Raman intensity of graphitic materials as a function of laser energy and crystallite size. *Chemical Physics Letters* 2006; 427(1-3): 117–21. doi:10.1016/j.cplett.2006.05.107.
- [54] Ferrari AC, Robertson J. Interpretation of Raman spectra of disordered and amorphous carbon. *Phys. Rev. B* 2000; 61(20): 14095–107. doi:10.1103/PhysRevB.61.14095.
- [55] Ferrari AC. Raman spectroscopy of graphene and graphite: Disorder, electron–phonon coupling, doping and nonadiabatic effects. *Solid State Communications* 2007; 143(1-2): 47–57. doi:10.1016/j.ssc.2007.03.052.
- [56] Tuinstra F, Koenig JL. Characterization of Graphite Fiber Surfaces with Raman Spectroscopy. *Journal of Composite Materials* 1970; 4(4): 492–9. doi:10.1177/002199837000400405.
- [57] Tuinstra F, Koenig JL. Raman Spectrum of Graphite. *J. Chem. Phys.* 1970; 53(3): 1126–30. doi:10.1063/1.1674108.
- [58] Jäger H, Cherif C, Kirsten M, Behnisch T, Wolz DS, Böhm R et al. Influence of processing parameters on the properties of carbon fibres – an overview. *Materialwissenschaft und Werkstofftechnik* 2016. doi:10.1002/mawe.201600630.
- [59] Toray Industries. TORAYCA® yarn: Product lineup. [August 2018]; Available from: http://www.torayca.com/en/lineup/product/pro_001.html.